Electrical Spin Injection and Threshold Reduction in a Semiconductor Laser

M. Holub, J. Shin, D. Saha, and P. Bhattacharya

Solid-State Electronics Laboratory, Department of Electrical Engineering and Computer Science, University of Michigan, Ann Arbor, Michigan 48109-2122, USA

(Received 26 September 2006; published 5 April 2007)

A spin-polarized vertical-cavity surface-emitting laser is demonstrated with electrical spin injection from an $Fe/Al_{0.1}Ga_{0.9}As$ Schottky tunnel barrier. Laser operation with a spin-polarized current results in a maximum threshold current reduction of 11% and degree of circular polarization of 23% at 50 K. A cavity spin polarization of 16.8% is estimated from spin-dependent rate equation analysis of the observed threshold reduction.

DOI: 10.1103/PhysRevLett.98.146603 PACS numbers: 72.25.Hg, 42.55.Px, 72.25.Mk, 72.25.Pn

Spin-polarized lasers are expected to outperform semiconductor lasers whose operation depends solely on electron charge. Spin-dependent effects such as ultrafast optical switching [1], polarization control [2], and threshold current reduction [3] have already been demonstrated in vertical-cavity surface-emitting lasers (VCSELs) using circularly polarized photoexcitation to generate spin-polarized carriers. The ability to independently modulate the optical polarization and intensity in spin-polarized VCSELs (spin-VCSELs) make these lasers suitable for a wide range of applications, including reconfigurable optical interconnects, ultrafast optical switches, chiroptical spectroscopy, and telecommunications with enhanced bandwidth.

Spin-VCSEL operation stems from optical selection rules which govern the conversion between spin and photon angular momentum [4]. [Recombination of spin-up (spin-down) electrons and heavy holes radiates left-hand (right-hand) circularly polarized photons.] The fundamental mode of a VCSEL may be described by two, circularly polarized lasing transitions in which intermixing occurs through spin-flip processes [5], and spin-polarized carriers will couple selectively to one circularly polarized mode to satisfy angular momentum conservation. A randomly polarized current will feed both modes equally such that both modes must reach threshold for lasing to occur. Consequently, both modes radiate equal intensities which admix above threshold to form linearly polarized emission. A spin-polarized current, however, will feed one mode preferentially such that the favored mode can reach threshold with fewer total carriers. Lasing of the unfavored mode is effectively suppressed until the injection current is increased sufficiently to satisfy lasing requirements for both circularly polarized modes. The onset of lasing occurs with fewer total carriers as required for a randomly polarized current, and the overall threshold current of the laser is effectively reduced. Injection of a 100% spin-polarized current is expected to result in a theoretically maximal reduction of 50%.

Threshold current reductions have been demonstrated experimentally in optically pumped spin-VCSELs at both low and room temperature [3,6]. However, electrically pumped spin lasers are essential for practical applications. Confirmation of electrical spin injection in VCSELs is nontrivial and complicated by a need to apply large magnetic fields to perpendicularly magnetize most thin-film ferromagnets [7]. In this Letter, we report the first unambiguous demonstration of an electrically pumped spin-VCSEL where an Fe Schottky tunnel contact is utilized for electron spin injection into an InGaAs quantum well (QW) VCSEL. A net degree of circular polarization of 23% along with a significant threshold current reduction of 11% are observed. Rate equation analysis of the observed reduction provides a reasonable estimate of the cavity spin polarization.

The laser sample is grown by molecular-beam epitaxy (MBE) and consists of a 29.5-pair $Al_{0.8}Ga_{0.2}As/GaAs$ distributed Bragg reflector (DBR) stack for the bottom mirror, a full-wave GaAs cavity with an $In_{0.2}Ga_{0.8}As$ multiple QW (MQW) active region, and a hybrid top mirror formed from one quarter-wave pair of p-doped ($N_A = 5 \times 10^{18}$ cm^{-3}) $Al_{0.8}Ga_{0.2}As/GaAs$ DBR and a 5-pair $MgF_2/ZnSe$ dielectric DBR stack [7]. For the bottom DBR mirror, only the three $Al_{0.8}Ga_{0.2}As/GaAs$ pairs nearest to the cavity are n-doped ($N_D = 7 \times 10^{17}$ cm^{-3}). Circular post spin-VCSELs are fabricated using standard microfabrication techniques. We elect annular intracavity contacts for electrical device connection which are interconnected to coplanar anode and cathode bond pads. Such a configuration is commonly used in high-performance VCSELs. An $Fe/Al_{0.1}Ga_{0.9}As$ Schottky barrier is deposited by MBE regrowth around the laser mesas on the topmost n-GaAs layer, which is needed to reduce the transport length from the Fe contact to the active region. We adopt a recipe reported by Hanbicki *et al.* [8], which results in spin-injection efficiencies of $\sim$30% over the temperature range of 90–240 K. Control VCSELs where Fe is deposited atop nonmagnetic n-Ohmic metallization and nonmagnetic VCSELs containing no Fe are also fabricated to provide evidence of electrical spin injection in our Fe spin-VCSEL.

The polarization of VCSEL emission is determined by spin and cavity anisotropies, which can either compete or

cooperate to determine the laser polarization state [9]. Though cylindrically-symmetric VCSELs ideally lack a polarization anisotropy mechanism to select a preferred polarization, linearly polarized emission aligned along a ⟨110⟩ axis is generally observed and attributed to strain-induced birefringence [10]. This polarization preference is relatively weak, leading to polarization switching induced by changes in temperature, injection current, or stress. Measurements on our VCSELs find a highly linearly polarized emission above threshold with the polarization axis aligned along a ⟨110⟩ direction. In this experiment, we confirm that the spin anisotropy induced from spin injection can overcome unintentional polarization preferences present in our design.

The degree of circular polarization, Π_C, of the Fe spin-VCSEL is analyzed using a photoelastic modulator and linear polarizer combined with lock-in detection. The laser is biased near threshold [$1.2 \times I_{\mathrm{th},0}$ where $I_{\mathrm{th},0}$ is the threshold current at zero magnetic field ($H = 0$)] under continuous-wave (cw) operation and characterized using the Faraday geometry. As shown in Fig. 1(a), Π_C for a 15 μm diameter Fe spin-VCSEL is seen to very closely track the out-of-plane magnetization of a 10 nm Fe layer, which demonstrates that the electroluminescence polarization originates from the Fe contact. Π_C saturates at nearly 23% for applied magnetic fields greater than the out-of-plane saturation field for Fe ($H_{\mathrm{sat}} \simeq 2.2$ T), and the sign of Π_C is indicative of majority spin injection. Since spin injection results in a net circular polarization, we conclude

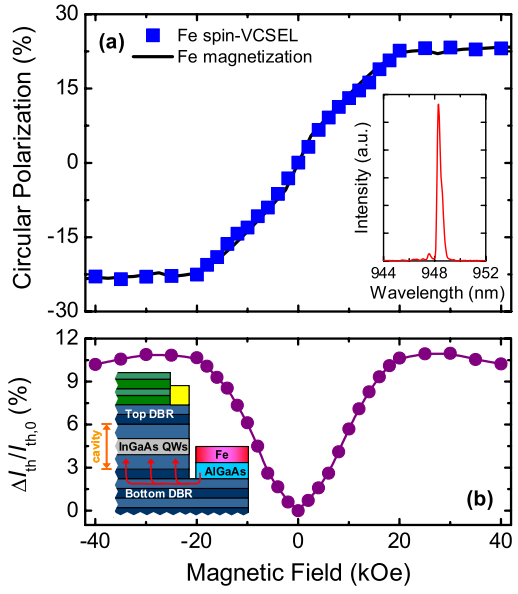

FIG. 1 (color online). (a) Degree of circular polarization and (b) threshold current reduction versus magnetic field for a 15 μm diameter spin-polarized VCSEL measured at 50 K. The normalized out-of-plane magnetization curve for a 10 nm Fe layer is shown for comparison. Top inset shows the electroluminescence spectrum, exhibiting a full-width at half maximum of 0.36 nm at 50 K. Bottom inset depicts the Fe spin-polarized VCSEL design.

that spin anisotropy is sufficient to overcome other anisotropy mechanisms introduced from cavity anisotropy, geometry, or wave guiding effects that impart a preference for linear polarization in the Fe spin-VCSEL.

Longitudinal and transverse optical confinement are ensured by the DBR mirrors and post geometry, respectively, such that the emission never passes through the ferromagnetic Fe layer. Therefore, a parasitic polarization arising from magnetic circular dichroism (MCD) is absent in our laser since the Fe layer is incorporated outside of the cylindrical resonator; this assumption is verified through magneto-photoluminescence measurements [11]. Moreover, a $\Pi_C < 1.5\%$ is measured for magnetic fields up to 40 kOe in the control VCSEL, which is significantly less than the saturation value of Π_C measured for the Fe spin-VCSEL. Parasitic contributions from stray field or magneto-optical effects cannot account for the observed Π_C in the Fe spin-VCSEL, which provides convincing evidence of spin injection, transport, and detection in our Fe spin-VCSEL.

Semiconductor lasers are expected to exhibit a threshold current reduction when pumped with a spin-polarized current. Any change in threshold current (ΔI_{th}) will be reflected by a change in total light intensity (ΔL) for a fixed current bias, and the threshold current reduction may be determined from $\Delta I_{\mathrm{th}} = \Delta L/\eta_D$, where η_D is the differential slope efficiency. Magnetic field dependent optical power measurements are performed in the Faraday geometry for cw-biased Fe spin-VCSELs. As H is increased from 0 to 40 kOe, an emission intensity enhancement and corresponding threshold current reduction are observed for a 15 μm diameter spin-VCSEL biased at $1.2 \times I_{\mathrm{th},0}$ [Fig. 1(b)]. The threshold current reduction saturates for $H > H_{\mathrm{sat}}$ at a value of 11%. The gradual decrease of $\Delta I_{\mathrm{th}}/I_{\mathrm{th},0}$ at high magnetic fields is attributed to the slight decrease in total light intensity with increasing magnetic field, which is observed for both spin-polarized and nonmagnetic VCSELs. The mechanism responsible for this behavior is currently unknown. Negligible threshold current reductions are observed for the control and nonmagnetic VCSELs [11]. This finding proves that the threshold current reduction results exclusively from electron spin injection by the Fe/AlGaAs Schottky tunnel barrier.

As shown in the inset to Fig. 1(b), placement of the spin injector around the laser mesa requires both transverse and longitudinal spin transport for electron spins to reach the laser active region. The separation between the Fe contact and laser mesa is $\sim$1 μm. This results in an average electron spin transport length of $\sim$4.5 μm in a 15 μm spin-VCSEL. The observation of a sizable threshold reduction is in accord with spin transport lengths exceeding 30 μm observed by other groups [12,13].

To analyze the carrier-photon dynamics in our Fe spin-VCSEL, we employ a rate equation model [3,6,14] which accounts for the spin-up and spin-down carrier densities in the barrier, $n_b^{\pm}$, and MQW active region, $n^{\pm}$, and the

photon density for right- and left-circularly polarized light, $S^{\pm}$. The rate equations are as follows:

$$\frac{\partial n_b^{\pm}}{\partial t} = -\frac{n_b^{\pm}}{\tau_{\mathrm{cap}}} + \frac{1 \pm P_{\mathrm{spin}}}{2}\frac{I_{\mathrm{pump}}}{qV_b} \mp \frac{n_b^{+} - n_b^{-}}{\tau_{s,b}},$$

$$\frac{\partial n^{\pm}}{\partial t} = \frac{V_b}{V_{\mathrm{MQW}}}\frac{n_b^{\pm}}{\tau_{\mathrm{cap}}} - v_g g(n^{\pm}, S^{\mp})S^{\mp} \mp \frac{n^{+} - n^{-}}{\tau_s} - B_{\mathrm{sp}}\frac{n^{\pm}(n^{+} + n^{-})}{2} - C\frac{n^{\pm}(n^{+} + n^{-})^2}{2}$$

$$\frac{\partial S^{\pm}}{\partial t} = \Gamma v_g g(n^{\mp}, S^{\pm})S^{\pm} + \Gamma\beta B_{\mathrm{sp}}\frac{n^{\mp}(n^{+} + n^{-})}{2} - \frac{S^{\pm}}{\tau_{\mathrm{ph}}},$$

where τ_{cap} is the carrier capture time, P_{spin} is the degree of spin polarization of the pump current (I_{pump}), τ_b (τ_s) is the spin-flip time in the barrier (QW), V_b (V_{MQW}) is the volume of the barrier (active region), B_{sp} (C) is the bimolecular radiative (Auger) recombination coefficient, v_g is the group velocity of light, Γ is the optical confinement factor, β is the spontaneous emission factor, and τ_{ph} is the photon cavity lifetime. The gain in the laser cavity is modeled as $g(n, S) = dg/dn(n - n_{\mathrm{tr}})/(1 + \epsilon S)$, where dg/dn is the differential gain, n_{tr} is the transparency carrier density, and ϵ is the gain compression factor. The parameters used in our analysis are estimated from reports on similar structures characterized at cryogenic temperatures and are as follows [15–22]: $\tau_{\mathrm{cap}} = 45$ ps, $\tau_{s,b} = 500$ ps, $\tau_s = 300$ ps, $dg/dn = 1.1 \times 10^{-14}$ cm/s, $n_{\mathrm{tr}} = (3.6 - 4.9) \times 10^{-17}$ cm^{-3}, $\epsilon = 4.5 \times 10^{-17}$ cm^3, $B_{\mathrm{sp}} = 9.4 \times 10^{-10}$ cm^3/s, $C = 3.8 \times 10^{-29}$ cm^6/s, $v_g = 0.87 \times 10^{10}$ cm/s, $\Gamma = 0.029$, $\beta = 6 \times 10^{-4}$, and $\tau_{\mathrm{ph}} = 1.25$ ps.

A P_{spin} of $\pm 19.8\%$ corresponds to a threshold current reduction of 11% for the 15 μm diameter Fe spin-VCSEL discussed above. Figures 2(a) and 2(b) show the light versus current (L-I) characteristics for $P_{\mathrm{spin}} = 0\%$ and -19.8%, respectively, where the total light intensity is the sum of the right-hand and left-hand circularly polarized lasing mode intensities. The threshold currents for the circularly polarized modes ($I_{\mathrm{th}}^{\pm}$) separate as P_{spin} increases, and the overall laser threshold current is determined by the favored mode. It can be seen in Fig. 2(b) that a kink in the L-I characteristics is introduced at an injection current value equal to the threshold current of the unfavored mode.

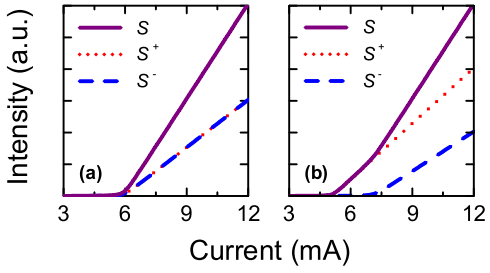

FIG. 2 (color online). Theoretical light versus current characteristics for a 15 μm spin-polarized VCSEL driven with (a) 0% and (b) -19.8% spin-polarized pump currents. The solid line represents the total light intensity, S, which is the summation of the right-hand (S^{+}, dotted line) and left-hand circularly polarized (S^{-}, dashed line) modes.

The electron spin polarization in the GaAs barrier ($\Pi_{S,b}$) and InGaAs MQW active region (Π_S) corresponding to $P_{\mathrm{spin}} = -19.8\%$ and evaluated at threshold are approximately -16.8% and -7%, respectively. The barrier spin polarization is found to be essentially independent of bias, determined primarily by P_{spin}, $\tau_{s,b}$, and τ_{cap}. In stark contrast, the quantum well spin polarization is influenced by the value of $g(n^{\pm}, S^{\mp})$ and therefore depends strongly on bias. As the pump current increases, Π_S is seen from the rate equations to decrease rapidly from -7% at $I_{\mathrm{pump}} = I_{\mathrm{th}}^{+}$ to $\sim 0\%$ at $I_{\mathrm{pump}} \geq I_{\mathrm{th}}^{-}$. This phenomenon occurs since the carrier density for either mode above threshold is essentially fixed at the threshold carrier density. Any additional carriers recombine instantaneously—within the stimulated recombination lifetime—producing stimulated photons. For a pump current $I_{\mathrm{pump}} > I_{\mathrm{th}}^{-} > I_{\mathrm{th}}^{+}$, both circularly polarized modes are lasing and Π_S is negligibly small. The Fe spin-VCSEL circular polarization will instead be determined by $\Pi_{S,b}$ ($\sim 16.8\%$ for $H > H_{\mathrm{sat}}$).

According to optical selection rules, the degree of electron spin polarization in the active region corresponds to half the degree of circular polarization in bulk material and matches that in quantum wells. While these simple linear relationships hold for spin-polarized light-emitting diodes (spin-LEDs), they are invalid for spin VCSELs when biased above threshold due to optical amplification. A narrow injection current window exists in which the spin-induced gain anisotropy results in large degrees of circular polarization, even for small spin polarizations, through stimulated emission amplification. This effect is demonstrated in our Fe spin-VCSEL for which we measured a Π_C (23%) larger than the cavity spin polarization estimated from the observed threshold reduction (16.8%).

Because of the spin-induced gain anisotropy and resulting threshold reduction, a spin-VCSEL is expected to exhibit an increase in optical power for a given bias current under spin-polarized pumping. Here we define the emission intensity enhancement as $\bar{S} = (S + S_0)/S_0$, where S_0 is the total light intensity at $H = 0$. Figure 3 shows the bias and temperature dependence of $\bar{S}$ for a separate 15 μm diameter Fe spin-VCSEL under 4.5 kOe. The transparency carrier density is set to 4.9×10^{17}, 4.4×10^{17}, and 3.6×10^{17} cm^{-3} in order to match the threshold current measured at 50, 75, and 100 K, respectively. We calculate $\bar{S}$ at these temperatures where P_{spin} is used as the only fitting parameter. Excellent agreement between the experimental and theoretical values of $\bar{S}$ is found at 50, 75, and 100 K for pump current (cavity) spin polarizations of 5.3% (4.5%), 5.0% (4.2%), and 5.0% (4.2%), respectively. It is evident that $\bar{S}$ peaks at $I_{\mathrm{th},0}$ where switching from an unpolarized to a spin-polarized current can effectively switch the laser between stimulated and spontaneous emission regimes—a form of spin-controlled laser modulation. A discrepancy

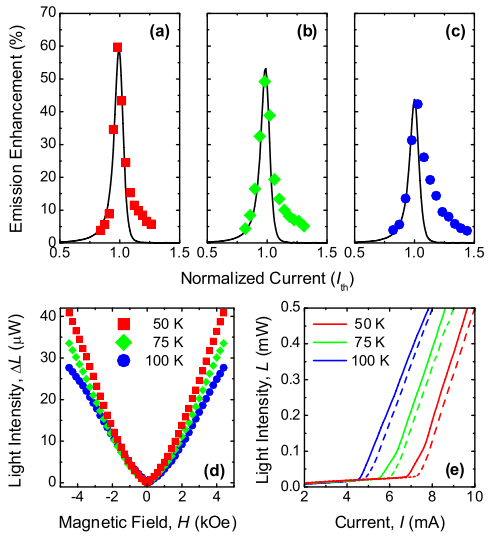

FIG. 3 (color online). Emission intensity enhancement versus normalized current (I/I_{th}) measured at (a) 50, (b) 75, and (c) 100 K for a 15 μm diameter Fe spin-polarized VCSEL under 4.5 kOe. The solid lines represent the emission intensity enhancement predicted from the rate equation analysis. (d) Light intensity change versus magnetic field and (e) light intensity versus current measured at 0 (dashed line) and 5 kOe (solid line).

between theory and experiment for $\bar{S}$ may be seen at high bias in Figs. 3(a)–3(c). The rate equations predict that the emission intensity for pump currents $I_{\mathrm{pump}} \geq \max\{I_{\mathrm{th}}^{+}, I_{\mathrm{th}}^{-}\}$ is the same regardless of the exact value for P_{spin}. We believe this to be a limitation of the model as higher emission intensities are experimentally observed well-above threshold under spin injection. Figures 3(d) and 3(e) show the change in total light intensity (ΔL) and the L-I characteristics, respectively, as a function of magnetic field. The large ΔL (tens of μW) resulting from the increase in slope efficiency with decreasing temperature enables measurement of small threshold current changes. The threshold current reductions at 4.5 kOe as inferred from Figs. 3(d) and 3(e) are 3.8%, 3.8%, and 3.6% at 50, 75, and 100 K, respectively. These values are in reasonable agreement with the reductions suggested from the L-I characteristics and from the rate equation model. The theoretically predicted kink in the L-I characteristics is observed experimentally [Fig. 3(e)] and is attributed to a separation of the circularly polarized lasing modes induced by electron spin injection.

We note that higher threshold current densities are measured for our 15 μm VCSELs than for larger mesa diameters, which is commonly observed in etched-posted VCSELs. Scattering and diffractive losses as well as surface recombination become dominant in small diameter etched-post VCSELs, causing the threshold gain to increase [23]. Threshold reductions reported here are measured for individual devices, so the precise value of the threshold current density is unimportant.

In conclusion, we have demonstrated electron spin injection from a Fe/AlGaAs Schottky tunnel barrier in an electrically pumped spin-VCSEL. A maximum threshold current reduction of 11% is observed in a 15 μm diameter spin-VCSEL with an electroluminescence circular polarization of 23%, from which a cavity spin polarization of 16.8% is estimated from a spin-dependent rate equation analysis.

This work is supported by the Office of Naval Research under Grant No. N00014-06-1-0025.

[1] S. Hallstein *et al.*, Phys. Rev. B **56**, R7076 (1997).
[2] H. Ando, T. Sogawa, and H. Gotoh, Appl. Phys. Lett. **73**, 566 (1998).
[3] J. Rudolph *et al.*, Appl. Phys. Lett. **82**, 4516 (2003).
[4] *Optical Orientation*, edited by F. Meier and B. P. Zakharchenya (Elsevier Science, Amsterdam, 1984).
[5] M. San Miguel, Q. Feng, and J. V. Moloney, Phys. Rev. A **52**, 1728 (1995).
[6] J. Rudolph *et al.*, Appl. Phys. Lett. **87**, 241117 (2005).
[7] M. Holub *et al.*, Appl. Phys. Lett. **87**, 091108 (2005); also see associated comment and reply.
[8] A. T. Hanbicki *et al.*, Appl. Phys. Lett. **80**, 1240 (2002).
[9] J. Martin-Regalado *et al.*, IEEE J. Quantum Electron. **33**, 765 (1997).
[10] A. K. J. van Doorn, M. P. van Exter, and J. P. Woerdman, Appl. Phys. Lett. **69**, 1041 (1996).
[11] See EPAPS Document No. E-PRLTAO-98-057715 for a heterostructure diagram of our spin-polarized VCSEL including the *n*-contact variations for the control devices. Results from control experiments which support and confirm the conclusions in our Letter are also included in this supplementary document. For more information on EPAPS, see http://www.aip.org/pubservs/epaps.html.
[12] M. Beck *et al.*, Europhys. Lett. **75**, 597 (2006).
[13] S. A. Crooker and D. L. Smith, Phys. Rev. Lett. **94**, 236601 (2005).
[14] R. Nagarajan *et al.*, IEEE J. Quantum Electron. **28**, 1990 (1992).
[15] L. V. Dao *et al.*, Appl. Phys. Lett. **73**, 3408 (1998).
[16] K. Jarasiunas *et al.*, Semicond. Sci. Technol. **19**, S339 (2004).
[17] K. Morita *et al.*, Physica (Amsterdam) **E21**, 1007 (2004).
[18] B. Dareys *et al.*, J. Phys. IV **3**, 351 (1993).
[19] L. F. Lester *et al.*, Appl. Phys. Lett. **59**, 1162 (1991).
[20] A. F. G. Monte *et al.*, J. Appl. Phys. **85**, 2866 (1999).
[21] S. Hausser *et al.*, Appl. Phys. Lett. **56**, 913 (1990).
[22] R. J. Ram *et al.*, IEEE Photonics Technol. Lett. **8**, 599 (1996).
[23] B. J. Thibeault *et al.*, J. Appl. Phys. **78**, 5871 (1995).